

3-Hydroxy-1,5-dihydro-pyrrol-2-one derivatives as advanced inhibitors of HIV integrase

Takashi Kawasuji,^{a,*} Masahiro Fuji,^a Tomokazu Yoshinaga,^b Akihiko Sato,^b
Tamio Fujiwara^b and Ryuichi Kiyama^a

^aShionogi Research Laboratories, Shionogi & Company, Ltd, Sagisu, Fukushima-ku, Osaka 553-0002, Japan

^bShionogi Research Laboratories, Shionogi & Company, Ltd, Mishima, Settsu-shi, Osaka 556-0022, Japan

Received 17 April 2007; revised 16 May 2007; accepted 19 May 2007

Available online 25 May 2007

Abstract—The two-metal binding model we previously reported as an inhibition mechanism of HIV integrase (HIV IN) produced a new direction in modification of 2-hydroxy-3-heteroaryl acrylic acid inhibitors (HHAAs). Here we present a novel series of HIV IN inhibitors having a 3-hydroxy-1,5-dihydro-pyrrol-2-one moiety (HDPO) as an advanced analog of HHAAs. This cyclic modification of the chelating region of HHAA produces a favorable configuration to coordinate two-metal ions in HIV IN, which consequently gave improvements in not only enzymatic assay but also antiviral cell based assay in many cases.

© 2007 Elsevier Ltd. All rights reserved.

1. Introduction

2,4-Diketo-butanoic acid derivatives¹ (DKAs), which have been identified as inhibitors of HIV IN² and viral replication, are still attractive lead analogs in this field. In particular S-1360 depicted in Figure 1 has potent activity not only in the enzymatic assays but also in the antiviral assay, and was the first integrase inhibitor to progress into clinical development.³ We previously reported 2-hydroxy-3-heteroaryl acrylic acid derivatives (HHAAs) which were designed from DKAs as inhibitors of HIV IN.⁴ The general structure of HHAAs consists of a 2-hydroxy acrylic acid substructure and a nitrogen-containing heteroaromatic ring connected with a hydrophobic substituent, for example, a benzyloxy group. Combinations of heteroaromatic and hydrophobic substituents connecting on different positions gave drastic changes in the structure–activity relationships (SARs), which were studied using molecular modeling techniques, and finally showed some pharmacophore features critical for activity. For the hydrophilic domain of HHAAs, all hydrophilic functional groups were very important to show inhibitory activity. We also proposed the two-metal binding model as a relevant mechanism of

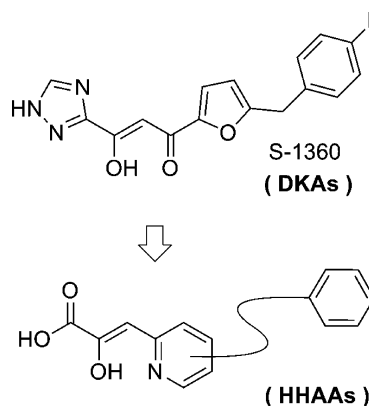


Figure 1. Design of HHAAs from DKAs (previous work⁴).

the HHAAs against HIV IN.⁵ The model indicates that potential inhibitors would bind to two-metal ions in the active site of HIV IN to prevent human DNAs from undergoing the integration reaction as shown in Figure 2a. This theory was supported by a metal titration study and a modeling study. HHAAs showed high inhibitory activities in MWPA–Mn enzymatic assay using Mn²⁺ cofactor, but lower activities in MWPA–Mg assay using Mg²⁺ cofactor, because of lower affinity to Mg²⁺. The HHAAs are inactive in antiviral cell based assay in which HIV IN works with Mg²⁺ cofactors (compound 1 in Table 1).² This indicates that they

Keywords: HIV integrase; Two-metal binding model; Chelating inhibitor.

* Corresponding author. Fax: +81 6 6458 0987; e-mail: takashi.kawasuji@shionogi.co.jp

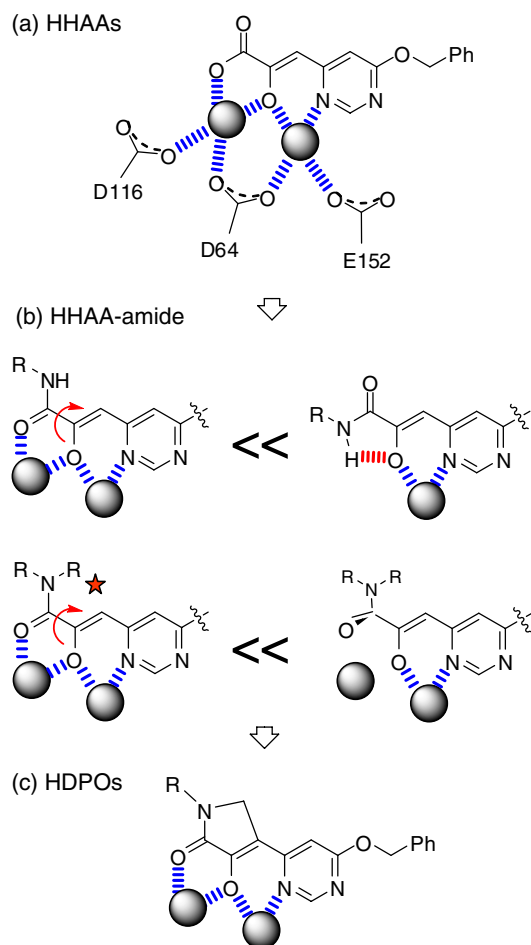


Figure 2. Process of drug design from HHAAs to HDPOs (this work). (a) Two-metal binding model of HHAAs. D64, D116, and E152 indicate catalytic triad of HIV IN. The blue dashed line represents coordination to the metal ion depicted as a gray sphere. (b) Explanations of why HHAA-amide derivatives do not show potential activity. The sign of inequality indicates likelihood of the conformational change. The red star is attached around the site where the unfavorable intramolecular repulsion can be observed. The red dashed line is an intramolecular hydrogen bond. The red curved arrow indicates the bond which would be rotated by the unfavorable intramolecular repulsion or hydrogen bonding. (c) Designed structure of HDPOs. The methylene bridging modification forces the amide oxygen to face the favorable direction to coordinate to the metal ion.

Table 1. Inhibitory activities of HHAA and HHAA-amide (previous work⁵)

Compound	R'	MWPA–Mn ^a (μM)	MWPA–Mg ^a (μM)	MTT EC ₅₀ ^b (μM)
1	–OH	0.037	9.6	34
2a	–NH ₂	71	6.7	49
2b	–NHMe	39	11	24
2c	–Morpholine	262	236	>59

^a IC₅₀ against the strand transfer. Different metal cofactors were used for each method.

^b Anti-HIV activities, see Refs. 4 and 5 for details of the assays.

should have a positive effect in MWPA–Mg rather than MWPA–Mn in respect to antiviral activity. From this perspective the amide derivatives **2a** and **2b** (HHAA-amide) showed low but interesting activity in not only MWPA–Mg but also the antiviral MTT assay despite the low activities in the MWPA–Mn assay. This feature was never seen in the other HHAAs reported, and it should be realized as an attractive lead analog for improving the antiviral activity.

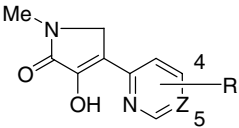
Each heteroatom participating in chelation should be arranged to face the same way to chelate the adjoining two-metal ions, and the chelating region of an inhibitor should be planar to point each lone-pair toward the metal, which is consistent with the two-metal inhibition model and explains why the HHAA-amide showed only weak inhibitory activity. The amide regions show an unfavorable intramolecular hydrogen bonding or repulsion, preventing construction of 5,6-parallel chelating system as shown in Figure 2b. To counter this structural issue we produced a 3-hydroxy-1,5-dihydro-pyrrol-2-one moiety (HDPO) for replacement of the HAA region of HHAAs as shown in Figure 2c. In brief, the nitrogen atom of the HHAA-amide ties to the carbon position 3 with a bridge. By doing this, the amide oxygen can be fixed to face the favorable direction to coordinate to the metal ion. Though several kinds of bridge could be designed, we incorporated a methylene (–CH₂–) for two main reasons. First a mesomeric or electrostatic effect by an unsaturated or heteroatomic bridge might have an unexpected influence on the chelating feature of the amide, and second a six- or more-membered cyclic system by a saturated bridge causes an unfavorable contortion of the chelating region because of a complexity of cyclic configurations or repulsion with neighboring groups. The compounds modified based on HHAAs are referred to as HHAA–HDPOs. In this paper, we present the same HDPO modification on S-1360 representing DKAs, those are referred to as DKA–HDPOs. The effect of substituents on the HDPO's nitrogen is also presented.

2. Chemistry

All HHAA–HDPOs in Tables 2 and 3 were prepared from the corresponding ester precursors⁴ of HHAAs as shown in Scheme 1. The ester **3** was treated with para-formaldehyde and corresponding primary amine to give the desired compound **4**. All DKA–HDPOs in Table 4 were prepared from the corresponding ester derivative⁵ of S-1360 (compound **5** in Scheme 1) in the same manner as the HHAA–HDPOs.

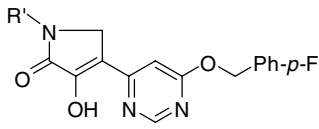
3. Biological results and discussion

The results of the HHAA–HDPOs with the methyl group on HDPO's nitrogen are listed in Table 2 along with those of corresponding HHAAs. The 5-substituted HHAA–HDPOs (**4a–c**) show one or two orders of magnitude improvement compared to the corresponding HHAAs (**7a–c**) in MWPA–Mg and also antiviral assay.

Table 2. The data of HHAA–HDPOs comparing to the corresponding HHAA on inhibitory activities in enzyme and anti-HIV assay


Compound	Z ^a	Position ^b	R	MWPA–Mn ^c (μM)	MWPA–Mg ^c (μM)	MTT EC ₅₀ ^d (μM)
4a (7a)	C	5	–OCH ₂ Ph- <i>p</i> -F	<0.021 (0.066)	0.030 (0.48)	0.18 (45.7)
4b (7b)	C	5	–CH ₂ Ph- <i>p</i> -F	<0.021 (0.095)	0.037 (1.4)	0.17 (8.8)
4c (7c)	C	5	–OPh- <i>p</i> -F	<0.021 (0.11)	0.08 (8.7)	1.9 (>73)
4d (7d)	N	4	–CH ₂ CH ₂ Ph- <i>p</i> -F	0.32 (0.059)	0.32 (1.8)	0.80 (27)
4e (7e)	N	4	–OCH ₂ Ph- <i>p</i> -F	0.30 (0.014)	0.063 (0.093)	0.32 (7.9)

Data of the corresponding HHAA in parentheses.

^a ‘C’ and ‘N’ indicate carbon and nitrogen, respectively.^b The substituted position of R group.^c IC₅₀ against the strand transfer. Different metal cofactors were used for each method.^d Anti-HIV activities.**Table 3.** Effect of a substituent on HDPO's nitrogen for HHAA–HDPOs


Compound	R'	MWPA–Mg ^a (μM)	MTT EC ₅₀ ^b (μM)
4f	H	0.040	0.24
4g	Hydroxyethyl	0.046	0.38
4h	Methoxyethyl	0.053	0.47
4i	<i>i</i> -Propyl	0.082	1.4
4j	<i>n</i> -Propyl	0.27	9.0
4k	<i>p</i> -Methoxybenzyl	0.14	3.3

^a IC₅₀ against the strand transfer.^b Anti-HIV activities.

Comparison of the 4-substituted HHAA–HDPOs (**4d**, **e**) with the corresponding HHAA (**7d**, **e**) showed a small improvement in MWPA–Mg and about one order of magnitude improvement in antiviral assay. Contrarily about one order of magnitude less activity was observed in MWPA–Mn. The HDPO-modification for inactive HHAA previously⁴ reported produced only 2- to 3-fold of improvement in both enzymatic assays (data not shown).

The effect of substituents on HDPO's nitrogen was studied using compound **4e** as a model substrate of the HHAA–HDPOs as summarized in Table 3. Compound **4f** (R' = H) showed slight improvement in comparison to **4e** in enzymatic and antiviral assay. Other hydrophilic substituents, hydroxyethyl and methoxyethyl group (**4g**, **h**), gave no effect or slight reduction in activity. Obvious losses of activity were observed in the case of hydrophobic substituents as represented by compounds **4i–k**. Small and hydrophilic groups seem to be preferred for the substitution. The results of DKA–HDPOs with several substituents are listed in Table 4. The DKA–HDPOs showed potential activity in both enzymatic and antiviral assay, however some disadvantage can be observed compared to S-1360 in both assays. One possible reason for the loss of activity is that the methylene bridge and the hydrogen atom on the furan ring make close contact with each other, which might bring an unfavorable conformation change of the hydrophobic domain. Though only a small range in activity in enzymatic assay is observed among all R' substituents, a compact group like methyl or *i*-propyl group (**6b**, **c**) seems to be preferred for antiviral activity. On the contrary, hydrophilic functional groups like hydroxyethyl or morpholinoethyl (**6g**, **i**) and hydrophobic aromatic groups like *p*-methoxyphenyl or benzyl (**6f**, **h**) showed some loss of antiviral activity. The substituent on the HDPO's nitrogen is not so important for inhibitory

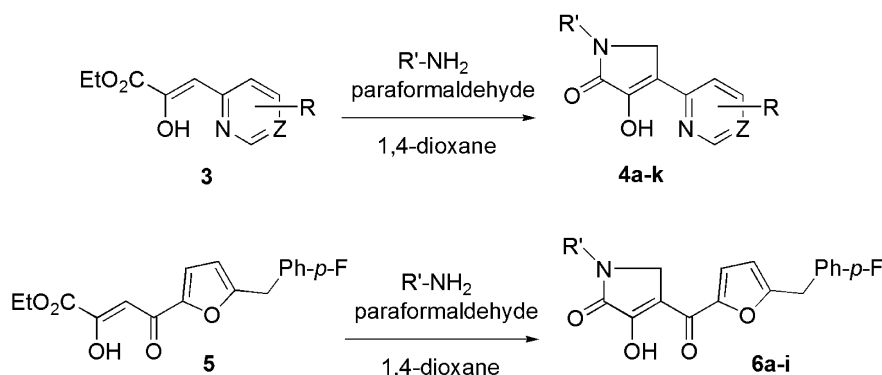
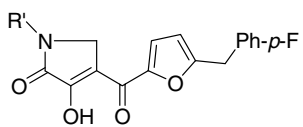
**Scheme 1.** Preparations of HHAA–HDPOs and DKA–HDPOs.

Table 4. Effect of a substituent on HDPO's nitrogen for DKA–HDPOs


Compound	R'	MWPA–Mg ^a (μM)	MTT EC ₅₀ ^b (μM)
S-1360			0.2
6a	H	0.10	0.93
6b	Methyl	0.082	0.63
6c	<i>i</i> -Propyl	0.079	0.55
6d	Methoxyethyl	0.16	0.67
6e	<i>c</i> -Pentyl	0.13	1.5
6f	<i>p</i> -Methoxyphenyl	0.17	13
6g	Hydroxyethyl	0.075	5.5
6h	Benzyl	0.18	7.4
6i	Morpholinoethyl	0.18	3.4

^a IC₅₀ against the strand transfer.^b Anti-HIV activities.

activity, but slightly affects the antiviral activity in general. The most significant impact on antiviral activity may be dependent on cell membrane permeability caused by different R' substituents.

4. Conclusions

We found HDPOs to show high inhibitory activity of HIV IN based on HHAs and the two-metal binding model. The HDPO replacement of the 2-hydroxy-acrylic acid region produced remarkable improvement in the enzyme assays and the anti-HIV assay in comparison to the corresponding HHAs. The HDPO modification on S-1360 representing DKAs was not effective. Variation of a substituent on the HDPO's nitrogen did not affect their activity, which suggests that this site is not surrounded tightly by any other cooperating molecules other than water when the inhibitors bind to HIV IN. This gives no contradiction with respect to the structural binding model of inhibitors and HIV IN core domain previously⁵ reported.

5. Experimental

5.1. Chemistry

¹H NMR spectra were determined as 300 MHz. All reactions were carried out under a nitrogen atmosphere with anhydrous solvents that had been dried over 4 Å molecular sieves.

5.2. Preparation of HDPO derivatives (4a–k, 6a–i)

5.2.1. 4-(6-(4-Fluorobenzoyloxy)pyrimidin-4-yl)-3-hydroxy-1-methyl-1H-pyrrol-2(5H)-one (4e). Paraformaldehyde (160 mg, 4 mmol) and methyl amine (0.31 mL, 40% in methanol, 4 mmol) were added to 3-[6-(4-fluorobenzoyloxy)-pyrimidin-4-yl]-2-hydroxy-acrylic acid ethyl ester (637 mg, 2 mmol) in 1,4-dioxane (7 mL) at room

temperature. The reaction mixture was stirred for 2 h, then diluted with a saturated aqueous solution of NH₄Cl and EtOAc. The organic layer was washed with water and brine, then dried over Na₂SO₄. The solvent was removed in vacuo. The precipitate was washed with *n*-hexane to give the product as pale yellow crystals (460 mg, 73% yield). Mp 222–224 °C, ¹H NMR (CDCl₃) δ 3.15 (s, 3H), 4.07 (s, 2H), 5.43 (s, 2H), 6.45 (s, 1H), 7.00–7.11 (m, 2H), 7.40–7.46 (m, 2H), 8.71 (s, 1H). Anal. Calcd for C₁₆H₁₄F₁N₃O₃: C, 60.95; H, 4.48; F, 6.03; N, 13.33. Found: C, 60.63; H, 4.15; F, 5.88; N, 13.24.

The following compounds were prepared in a similar manner to that described for **4e** from corresponding ester precursors and primary amines.

5.2.2. 4-(5-(4-Fluorobenzoyloxy)pyridin-2-yl)-3-hydroxy-1-methyl-1H-pyrrol-2(5H)-one (4a). Pale yellow crystals, 45% yield. Mp 210–211 °C, ¹H NMR (CDCl₃) δ 3.14 (s, 3H), 4.11 (s, 2H), 5.10 (s, 2H), 7.05–7.15 (m, 3H), 7.32 (dd, *J* = 9.0, 3.0 Hz, 1H), 7.38–7.45 (m, 2H), 8.29 (d, *J* = 3.0 Hz, 1H). Anal. Calcd for C₁₇H₁₅F₁N₂O₃: C, 64.96; H, 4.81; F, 6.06; N, 8.91. Found: C, 64.68; H, 4.77; F, 5.81; N, 8.78.

5.2.3. 4-(5-(4-Fluorobenzyl)pyridin-2-yl)-3-hydroxy-1-methyl-1H-pyrrol-2(5H)-one (4b). Pale yellow crystals, 37% yield. Mp 204–206 °C, ¹H NMR (CDCl₃) δ 3.14 (s, 3H), 3.97 (s, 2H), 4.12 (s, 2H), 6.98–7.16 (m, 5H), 7.53 (dd, *J* = 8.2, 2.1 Hz, 1H), 8.37 (d, *J* = 1.5 Hz, 1H). Anal. Calcd for C₁₉H₁₉F₁N₂O₂: C, 69.92; H, 5.87; F, 5.82; N, 8.58. Found: C, 69.74; H, 6.00; F, 5.72; N, 8.43.

5.2.4. 4-(5-(4-Fluorophenoxy)pyridin-2-yl)-3-hydroxy-1-methyl-1H-pyrrol-2(5H)-one (4c). Pale yellow crystals, 72% yield. Mp 229–230 °C, ¹H NMR (CDCl₃) δ 3.15 (s, 3H), 4.16 (s, 2H), 7.00–7.14 (m, 4H), 7.19 (d, *J* = 8.9 Hz, 1H), 7.50 (dd, *J* = 2.7, 8.5 Hz, 1H), 8.30 (d, *J* = 2.7 Hz, 1H). Anal. Calcd for C₁₆H₁₃F₁N₂O₃: C, 64.00; H, 4.36; F, 6.33; N, 9.33. Found: C, 63.90; H, 4.27; F, 6.13; N, 9.32.

5.2.5. 4-(6-(4-Fluorophenethyl)pyrimidin-4-yl)-3-hydroxy-1-methyl-1H-pyrrol-2(5H)-one (4d). Pale yellow crystals, 72% yield. Mp 225–228 °C, ¹H NMR (CDCl₃) δ 3.06 (s, 4H), 3.16 (s, 3H), 4.08 (s, 2H), 6.78 (s, 1H), 6.90–7.00 (m, 2H), 7.05–7.15 (m, 2H), 9.01 (s, 1H). Anal. Calcd for C₁₇H₁₆F₁N₃O₂: C, 65.17; H, 5.15; F, 6.06; N, 13.41. Found: C, 65.03; H, 5.31; F, 5.93; N, 13.37.

5.2.6. 4-(6-(4-Fluorobenzoyloxy)pyrimidin-4-yl)-3-hydroxy-1H-pyrrol-2(5H)-one (4f). Pale yellow crystals, 20% yield. Mp 196–196 °C, ¹H NMR (DMSO-*d*₆) δ 4.11 (s, 2H), 5.42 (s, 2H), 7.18–7.27 (m, 3H), 7.50–7.55 (m, 2H), 8.72 (s, 1H), 8.76 (t, *J* = 1.8 Hz, 1H). Anal. Calcd for C₁₅H₁₂F₁N₃O₃: C, 59.80; H, 4.01; F, 6.31; N, 13.95. Found: C, 59.53; H, 4.00; F, 6.21; N, 13.83.

5.2.7. 4-(6-(4-Fluorobenzoyloxy)pyrimidin-4-yl)-3-hydroxy-1-(2-hydroxyethyl)-1H-pyrrol-2(5H)-one (4g). Pale yellow crystals, 76% yield. Mp 178–180 °C, ¹H NMR (DMSO-*d*₆) δ 3.49 (t, *J* = 5.4 Hz, 2H), 3.59 (t, *J* = 5.3 Hz, 2H), 4.29 (s, 2H), 4.82 (br s, 1H), 5.42 (s, 2H), 7.18–7.27 (m,

3H), 7.50–7.55 (m, 2H), 8.75 (s, 1H). Anal. Calcd for $C_{17}H_{16}F_1N_3O_4$: C, 59.13; H, 4.67; F, 5.50; N, 12.17. Found: C, 59.07; H, 4.64; F, 5.55; N, 12.07.

5.2.8. 4-(6-(4-Fluorobenzyloxy)pyrimidin-4-yl)-3-hydroxy-1-(2-methoxyethyl)-1H-pyrrol-2(5H)-one (4h). Pale yellow crystals, 83% yield. Mp 153–154 °C, 1H NMR ($CDCl_3$) δ 3.35 (s, 3H), 3.59 (t, $J = 4.8$ Hz, 2H), 3.72 (t, $J = 4.8$ Hz, 2H), 4.23 (s, 2H), 5.43 (s, 2H), 6.49 (d, $J = 0.9$ Hz, 1H), 7.04–7.11 (m, 2H), 7.41–7.45 (m, 2H), 8.71 (d, $J = 0.9$ Hz, 1H). Anal. Calcd for $C_{18}H_{18}F_1N_3O_4$: C, 60.16; H, 5.05; F, 5.29; N, 11.69. Found: C, 60.17; H, 5.01; F, 5.37; N, 11.64.

5.2.9. 4-(6-(4-Fluorobenzyloxy)pyrimidin-4-yl)-3-hydroxy-1-isopropyl-1H-pyrrol-2(5H)-one (4i). Pale yellow crystals, 98% yield. Mp 191 °C, 1H NMR ($CDCl_3$) δ 1.25 (d, $J = 6.8$ Hz, 6H), 4.03 (s, 2H), 4.50–4.61 (m, 1H), 5.42 (s, 2H), 6.58 (d, $J = 0.9$ Hz, 1H), 7.05–7.11 (m, 2H), 7.40–7.45 (m, 2H), 8.72 (d, $J = 0.9$ Hz, 1H). Anal. Calcd for $C_{18}H_{18}F_1N_3O_3$: C, 62.97; H, 5.28; F, 5.53; N, 12.24. Found: C, 62.87; H, 5.11; F, 5.35; N, 12.05.

5.2.10. 4-(6-(4-Fluorobenzyloxy)pyrimidin-4-yl)-3-hydroxy-1-propyl-1H-pyrrol-2(5H)-one (4j). Pale yellow crystals, 78% yield. Mp 159–160 °C, 1H NMR ($CDCl_3$) δ 0.95 (t, $J = 7.5$ Hz, 3H), 1.66 (m, 2H), 3.51 (t, $J = 7.4$ Hz, 2H), 4.08 (s, 2H), 5.43 (s, 2H), 6.53 (d, $J = 0.9$ Hz, 1H), 7.05–7.11 (m, 2H), 7.40–7.45 (m, 2H), 8.71 (d, $J = 0.9$ Hz, 1H). Anal. Calcd for $C_{18}H_{18}F_1N_3O_3$: C, 62.97; H, 5.28; F, 5.53; N, 12.24. Found: C, 63.00; H, 5.24; F, 5.65; N, 12.21.

5.2.11. 4-(6-(4-Fluorobenzyloxy)pyrimidin-4-yl)-3-hydroxy-1-(4-methoxybenzyl)-1H-pyrrol-2(5H)-one (4k). Pale yellow crystals, 53% yield. Mp 227–228 °C, 1H NMR ($CDCl_3$) δ 3.78 (s, 3H), 3.91 (s, 2H), 4.66 (s, 2H), 5.40 (s, 2H), 6.38 (d, $J = 0.9$ Hz, 1H), 6.85–6.88 (m, 2H), 7.02–7.09 (m, 2H), 7.19–7.26 (m, 2H), 7.36–7.42 (m, 2H), 8.69 (d, $J = 0.9$ Hz, 1H). Anal. Calcd for $C_{23}H_{20}F_1N_3O_4 \cdot 0.1H_2O$: C, 65.27; H, 4.81; F, 4.49; N, 9.93. Found: C, 65.06; H, 4.52; F, 4.43; N, 9.94.

5.2.12. 4-(5-(4-Fluorobenzyl)furan-2-carbonyl)-3-hydroxy-1H-pyrrol-2(5H)-one (6a). Pale yellow crystals, 40% yield. Mp 178–179 °C, 1H NMR ($CDCl_3$) δ 4.05 (s, 2H), 4.39 (s, 2H), 6.30 (d, $J = 3.6$ Hz, 1H), 7.01–7.08 (m, 2H), 7.18–7.23 (m, 2H), 7.35 (d, $J = 3.6$ Hz, 1H). Anal. Calcd for $C_{16}H_{12}F_1N_1O_4 \cdot 0.3H_2O$: C, 62.66; H, 4.14; F, 6.19; N, 4.57. Found: C, 62.87; H, 4.29; F, 5.92; N, 4.17.

5.2.13. 4-(5-(4-Fluorobenzyl)furan-2-carbonyl)-3-hydroxy-1-methyl-1H-pyrrol-2(5H)-one (6b). Pale yellow crystals, 71% yield. Mp 141–142 °C, 1H NMR ($CDCl_3$) δ 3.13 (s, 3H), 4.08 (s, 2H), 4.12 (s, 2H), 6.29 (d, $J = 3.9$ Hz, 1H), 7.03–7.10 (m, 2H), 7.20–7.25 (m, 2H), 7.32 (d, $J = 3.9$ Hz, 1H). Anal. Calcd for $C_{17}H_{14}F_1N_1O_4$: C, 64.76; H, 4.48; F, 6.03; N, 4.44. Found: C, 64.73; H, 4.39; F, 5.80; N, 4.42.

5.2.14. 4-(5-(4-Fluorobenzyl)furan-2-carbonyl)-3-hydroxy-1-isopropyl-1H-pyrrol-2(5H)-one (6c). Pale yellow crystals, 68% yield. Mp 155–157 °C, 1H NMR ($CDCl_3$) δ 1.23 (d, $J = 6.6$ Hz, 6H), 4.08 (s, 2H), 4.13 (s, 2H),

4.52–4.58 (m, 1H), 6.33 (d, $J = 3.6$ Hz, 1H), 7.02–7.10 (m, 2H), 7.21–7.26 (m, 2H), 7.33 (d, $J = 3.6$ Hz, 1H). Anal. Calcd for $C_{19}H_{18}F_1N_1O_4 \cdot 0.2H_2O$: C, 65.77; H, 5.35; F, 5.48; N, 4.04. Found: C, 65.72; H, 5.27; F, 5.26; N, 3.97.

5.2.15. 4-(5-(4-Fluorobenzyl)furan-2-carbonyl)-3-hydroxy-1-(2-methoxyethyl)-1H-pyrrol-2(5H)-one (6d). Pale yellow crystals, 48% yield. Mp 105–106 °C, 1H NMR ($CDCl_3$) δ 3.36 (s, 3H), 3.60 (dd, $J = 5.2, 4.6$ Hz, 2H), 3.72 (dd, $J = 5.2, 4.6$ Hz, 2H), 4.06 (s, 2H), 4.40 (s, 2H), 6.29 (d, $J = 3.4$ Hz, 1H), 7.00–7.10 (m, 2H), 7.20–7.26 (m, 2H), 7.31 (d, $J = 3.7$ Hz, 1H). Anal. Calcd for $C_{19}H_{18}F_1N_1O_5$: C, 63.50; H, 5.05; F, 5.29; N, 3.90. Found: C, 63.39; H, 4.98; F, 5.20; N, 3.84.

5.2.16. 1-Cyclopentyl-4-(5-(4-fluorobenzyl)furan-2-carbonyl)-3-hydroxy-1H-pyrrol-2(5H)-one (6e). Pale yellow crystals, 79% yield. Mp 157–159 °C, 1H NMR ($CDCl_3$) δ 1.44–1.58 (m, 2H), 1.63–1.82 (m, 4H), 1.90–2.23 (m, 2H), 4.07 (s, 2H), 4.15 (s, 2H), 4.52–4.68 (m, 1H), 6.33 (d, $J = 3.6$ Hz, 1H), 7.01–7.07 (m, 2H), 7.19–7.23 (m, 2H), 7.33 (d, $J = 3.6$ Hz, 1H). Anal. Calcd for $C_{21}H_{20}F_1N_1O_4$: C, 68.28; H, 5.46; F, 5.14; N, 3.79. Found: C, 67.94; H, 5.48; F, 5.13; N, 3.72.

5.2.17. 4-(5-(4-Fluorobenzyl)furan-2-carbonyl)-3-hydroxy-1-(4-methoxyphenyl)-1H-pyrrol-2(5H)-one (6f). Pale yellow crystals, 17% yield. Mp 225–227 °C, 1H NMR ($CDCl_3$) δ 3.85 (s, 3H), 4.10 (s, 2H), 4.59 (s, 2H), 6.36 (d, $J = 3.6$ Hz, 1H), 6.96–7.00 (m, 2H), 7.02–7.10 (m, 2H), 7.20–7.28 (m, 2H), 7.39 (d, $J = 3.6$ Hz, 1H), 7.45–7.61 (m, 2H). Anal. Calcd for $C_{23}H_{18}F_1N_1O_5 \cdot 0.1H_2O$: C, 67.51; H, 4.48; F, 4.64; N, 3.42. Found: C, 67.31; H, 4.46; F, 4.38; N, 3.39.

5.2.18. 4-(5-(4-Fluorobenzyl)furan-2-carbonyl)-3-hydroxy-1-(2-hydroxyethyl)-1H-pyrrol-2(5H)-one (6g). Pale yellow crystals, 53% yield. Mp 144–146 °C, 1H NMR ($CDCl_3$) δ 3.68 (t, $J = 5.0$ Hz, 2H), 3.89 (t, $J = 5.0$ Hz, 2H), 4.07 (s, 2H), 4.37 (s, 2H), 6.29 (d, $J = 3.8$ Hz, 1H), 7.03–7.09 (m, 2H), 7.20–7.26 (m, 2H), 7.32 (d, $J = 3.8$ Hz, 1H). Anal. Calcd for $C_{18}H_{16}F_1N_1O_5$: C, 62.61; H, 4.67; F, 5.50; N, 4.06. Found: C, 62.39; H, 4.61; F, 5.42; N, 4.01.

5.2.19. 1-Benzyl-4-(5-(4-fluorobenzyl)furan-2-carbonyl)-3-hydroxy-1H-pyrrol-2(5H)-one (6h). Pale yellow crystals, 71% yield. Mp 129–130 °C, 1H NMR ($CDCl_3$) δ 3.99 (s, 2H), 4.13 (s, 2H), 4.71 (s, 2H), 6.27 (d, $J = 3.6$ Hz, 1H), 6.91–7.00 (m, 2H), 7.08–7.16 (m, 2H), 7.23–7.30 (m, 3H), 7.33–7.42 (m, 3H). Anal. Calcd for $C_{23}H_{18}F_1N_1O_4$: C, 70.58; H, 4.64; F, 4.85; N, 3.58. Found: C, 70.42; H, 4.56; F, 4.74; N, 3.60.

5.2.20. 4-(5-(4-Fluorobenzyl)furan-2-carbonyl)-3-hydroxy-1-(2-morpholinoethyl)-1H-pyrrol-2(5H)-one (6i). Pale yellow crystals, quantitative yield. Mp 189–190 °C, 1H NMR ($DMSO-d_6$) δ 3.00–3.80 (m, 12H), 4.08 (s, 2H), 4.14 (s, 2H), 6.37 (d, $J = 3.3$ Hz, 1H), 7.13–7.19 (m, 2H), 7.29–7.35 (m, 2H), 7.85 (br s, 1H). Anal. Calcd for $C_{22}H_{23}F_1N_2O_5 \cdot 0.3H_2O$: C, 62.94; H, 5.67; F, 4.53; N, 6.67. Found: C, 62.91; H, 5.61; F, 4.25; N, 6.64.

References and notes

1. Pais, G. C. G.; Burke, T. R., Jr. *Drugs Future* **2002**, 27, 1101–1111.
2. Chiu, T. K.; Davies, D. R. *Curr. Top. Med. Chem.* **2004**, 4, 965–979.
3. Yoshinaga, T.; Sato, A.; Fujishita, T.; Fujiwara, T. S-1360: In Vitro Activity of a New HIV-1 Integrase Inhibitor in Clinical Development. In *Ninth Conference on Retroviruses and Opportunistic Infections*, Seattle, Washington, USA, 24–28 February 2002. Abstracts, 55p, no. 8.
4. Kwasuji, T.; Yoshinaga, T.; Sato, A.; Yodo, M.; Fujiwara, T.; Kiyama, R. *Bioorg. Med. Chem.* **2006**, 14, 8430–8445.
5. Kwasuji, T.; Fuji, M.; Yoshinaga, T.; Sato, A.; Fujiwara, T.; Kiyama, R. *Bioorg. Med. Chem.* **2006**, 14, 8420–8429.